Korean J. Chem. Eng., 40(6), 1418-1424 (2023)
DOI: 10.1007/s11814-022-1330-x

pISSN: 0256-1115
eISSN: 1975-7220

High-efficiency oil/water separation of hydrophobic stainless steel Mesh filter through carbon and fluorine surface treatment

Seongjae Myeong*, Chaehun Lim*, Seokjin Kim*, and Young-Seak Lee*,,†**

*Department of Chemical Engineering and Applied Chemistry, Chungnam National University, 99 Daehak-ro, Yuseong-gu, Daejeon 34134, Korea
**Institute of Carbon Fusion Technology (InCFT), Chungnam National University, 99 Daehak-ro, Yuseong-gu, Daejeon 34134, Korea
(*Received 8 September 2022 • Revised 19 October 2022 • Accepted 31 October 2022*)

Abstract−With the rapid industrial development, the discharge of oily wastewater has increased and polluted the environment. The conventional oil/water separation method has problems, such as generating harmful by-products, high operating costs, and low efficiency. For this reason, research on the development of ideal oil/water separation materials is being actively conducted. In this work, a hydrophobic mesh filter with excellent separation efficiency and separation speed was prepared through the surface coating of stainless steel Mesh (SUS Mesh), which has a large aperture size. After carbon coating on the surface of the SUS Mesh using the physical vapor deposition method, hydrophobicity was improved by giving fluorine functional groups to the surface using fluorine plasma. The manufactured mesh filter separated the oil at a high flux (6,062 $Lm^{-2}h^{-1}$) in a horizontal condition without external force, and at a high speed of fewer than two minutes, with a separation efficiency is 99.88%. Very high separation efficiency was observed. In addition, the average efficiency of 99.77% was maintained even in continuous oil/water separation. The hydrophobic mesh filter fabricated by a simple process in this study can be evaluated as a promising oil/water separation material that can be actually applied to separate oil from oily wastewater.

Keywords: SUS Mesh, Surface Modification, Physical Vapor Deposition (PVD), Fluorine Plasma, Hydrophobic

INTRODUCTION

The development of industry and the advancement of living standards has increased industrial wastewater and domestic sewage oily wastewater discharge. Discharged in this way the oily wastewater causes environmental and economic problems [1-3]. Various methods, such as a combustion method, a decomposition method using a dispersant and a photocatalyst, and a separation method using gravity and centrifugal force are used to remove such oily wastewater [4-13]. However, these methods have disadvantages in environmental aspects, oil/water separation efficiency, and operating cost [14-17].

Among recent studies to overcome these shortcomings, a method using filtration materials separates water and oil into another space by filtering one of the oil or water and blocking the other in the oil/water mixture [14-19]. At this time, stainless steel mesh (SUS Mesh), fabrics, and polymeric membranes are used as substrate materials for Filtration [11,12,16,17]. Among them, SUS Mesh is inexpensive because it can be mass-produced, and has high stability and durability in water with strong mechanical properties and corrosion resistance. In addition, SUS Mesh can control the aperture size during the production process, so it is an advantageous material for controlling the permeation rate of wastewater compared to other materials [20,21]. However, the general SUS Mesh has the disadvantage of permeating both water and oil, so it is limited to use as filtration materials. Therefore, to use SUS Mesh as filtration material, it is necessary to change the wettability of SUS Mesh through surface modification.

Commonly used surface modifications are electrodeposition, hydrothermal route, chemical etching, in-situ growth, and dip coating [20-26]. These methods can change wettability by controlling the surface free energy and surface roughness of the SUS mesh. However, they are limited to industrial use due to their low stability and reuse, and their difficulty in uniformly reacting on all surfaces of SUS mesh despite the complicated process.

Meanwhile, the physical vapor deposition (PVD) method is one of the surface modification methods that can uniformly deposit inorganic and organic materials down to the nanoscale on the surface of various materials [27]. Carbon coating using the PVD method is one of the methods to increase the hydrophobicity of the material surface [28]. Recently, a method of further increasing the hydrophobicity has been studied to increase the utility of the carbon material, and the introduction of a fluorine functional group through fluorine plasma treatment is considered one of the effective methods. Fluorine plasma treatment is one of the simple surface treatment methods that can introduce fluorine functional groups to the surface of carbon materials with only a short reaction time [29-32]. -CF_2 and -CF_3 groups generated by fluorine plasma treatment on carbon materials greatly increase the hydrophobicity of the material because the surface free energy value is very low [33,

†To whom correspondence should be addressed.
E-mail: youngslee@cnu.ac.kr

34].

Therefore, this research manufactured mesh filters with improved hydrophobicity through fluorine plasma treatment after carbon coating by depositing pyrolysis fuel oil (PFO) on the surface of SUS mesh through the PVD method. Changes in the surface properties of mesh filters according to this manufacturing process were confirmed through XPS, Raman, and FE-SEM analysis, and the hydrophobicity change of the mesh filter surface was evaluated by measuring the water contact angle (WCA). In addition, selective separation capability for oil was evaluated and considered through self-manufactured oil/water separation equipment.

EXPERIMENTAL METHODS

1. Materials

In this study, a plain weave 304 stainless steel 20 mesh (Arimmesh Co., Korea) with an aperture size of 770 μm was used. The carbon precursor used in the PVD method was PFO (Yeocheon YNCC Co., Korea), and the fluorine plasma treatment was performed using high-purity CF_4 gas (99%, Deokyang Co., Korea). To examine the oil/water separation performance, oil/water separation equipment was manufactured, and the oil/water separation ability was evaluated using DI water and soybean oil (CJ CheilJedang Corp., Korea). A schematic diagram of the manufactured oil/water separation equipment is shown in Fig. S1.

2. Carbon Coating through PVD Method

To coat the SUS mesh with carbon, SUS mesh (60×60 mm) and PFO (5 g) were put inside the reactor, and carrier gas (N_2) was added at a rate of 100 sccm to react. The PFO is a petroleum residue oil that has abundant polycyclic aromatic hydrocarbons. In PFO with a low molecular weight distribution of 200 g/mol, most of the aromatic components are volatilized at less than 400 °C [27,35]. Therefore, in this experiment, the temperature inside the reactor was raised to 400 °C at a rate of 5 °C/min and maintained at 400 °C for 1 h to deposit volatilized PFO on SUS Mesh. Then, to carbonize the deposited PFO, the temperature was raised to 950 °C at a rate of 10 °C/min and maintained at 950 °C for 1 h to prepare a carbon-coated SUS Mesh. At this time, the carbon-coated SUS Mesh was named Mesh@C.

3. CF_4 Plasma Treatment

A plasma reactor (COGRADE, Femto Science Co., Korea) having a size of 250 * 300 * 200 mm was used to introduce fluorine functional groups into Mesh@C. The carbon-coated SUS Mesh was positioned 20 mm from the electrode, the inside of the reactor was decompressed to a vacuum state using a decompression pump, and then CF_4 gas was injected to react. Frequency, power, and flow rate were fixed at 60 kHz, 80 W, and 80 sccm, and the reaction time was changed to 1, 2, and 3 min. The mesh filters prepared according to the reaction times of 1, 2 and 3 min were named Mesh@C-F01, Mesh@C-F02, and Mesh@C-F03, respectively.

4. Characterization

To observe changes in surface properties, the surface morphological structure was examined using the Field employment scanning electron microscope (FE-SEM, Hitachi S-4800, Hitachi, Japan), and the atomic composition introduced on the surface was identified with energy dispersive X-ray spectroscopy (EDS, Ultim Max, OFORD, England). All observations were carried out without a metal coating at a high acceleration voltage of 10 kV with spot intensity 30. X-ray photoelectron spectroscopy (XPS, K-alpha+, Thermofisher, USA) analysis was performed to confirm the change in chemical properties during the manufacturing process of mesh filters. The XPS spectra were recorded by a monochromatic Al Kα radiation (1,486.6 eV). The spectra were obtained in the range from 0 to 1,200 eV, with the instrumental resolution of 1.0 eV at a pass energy of 100 eV. In addition, Raman spectroscopy (LabRAM HR-800, HORIBA, Japan) analysis was performed to examine the structural change of the coated carbon according to the fluorine plasma treatment time after carbon coating. To evaluate the surface wettability of the prepared mesh filters, the water contact angle of each sample was measured using a contact angle analyzer (Phoenix 300, Surface Electro Optics Co. Ltd, Korea). For each condition, 5-8 μL of DI water was dropped ten times to measure WCA, and the average value of the WCAs was obtained.

5. Selective Separation Ability for Oil

To evaluate the oil/water separation ability of the prepared mesh filters, an oil/water separation equipment was manufactured, and an experiment was conducted to separate DI water and soybean oil. As shown in Fig. S1(a), the oil/water separation equipment divided two baths with a mesh filter and placed them horizontally. As shown in Fig. S1(a), the oil/water separation equipment was divided two baths with a mesh filter and placed horizontally. At this time, the experiment was conducted until additional oil/water separation did not proceed.

The oil/water separation ability of the manufactured mesh filters was evaluated by the separation yield and separation efficiency. After the oil/water separation experiment, the purity of DI water in the solution remaining in the right bath was defined as the separation yield. And the purity of the oil in the solution obtained through the outlet was defined as the separation efficiency. At this time, the purity of water and oil was calculated using Eq. (1) and Eq. (2).

$$\text{Water purity } \eta\,(\text{wt\%}) = \left(1 - \frac{m_f}{m_0}\right) \times 100 \tag{1}$$

$$\text{Oil purity } \eta\,(\text{wt\%}) = \frac{m_f}{m_0} \times 100 \tag{2}$$

where, m_0 and m_f are the weight of the obtained solution and the weight of the solution after evaporating DI water by heating the solution. The solution was heated and stirred at 180 °C for 24 h using a heating stirrer.

Also, the flux of the solution passing through the prepared mesh filters was calculated using Eq. (3).

$$\text{Flux } (\text{L m}^{-2}\text{h}^{-1}) = \frac{V}{S \times \Delta t} \tag{3}$$

where, V is the volume of the separated solution, S is the area of the mesh filter through which the solution has passed, and Δt is the time taken until the separation of oil and DI water is no longer observed.

In addition, to test the continuous oil/water separation ability, an experiment was performed to separate oil and DI water ten times

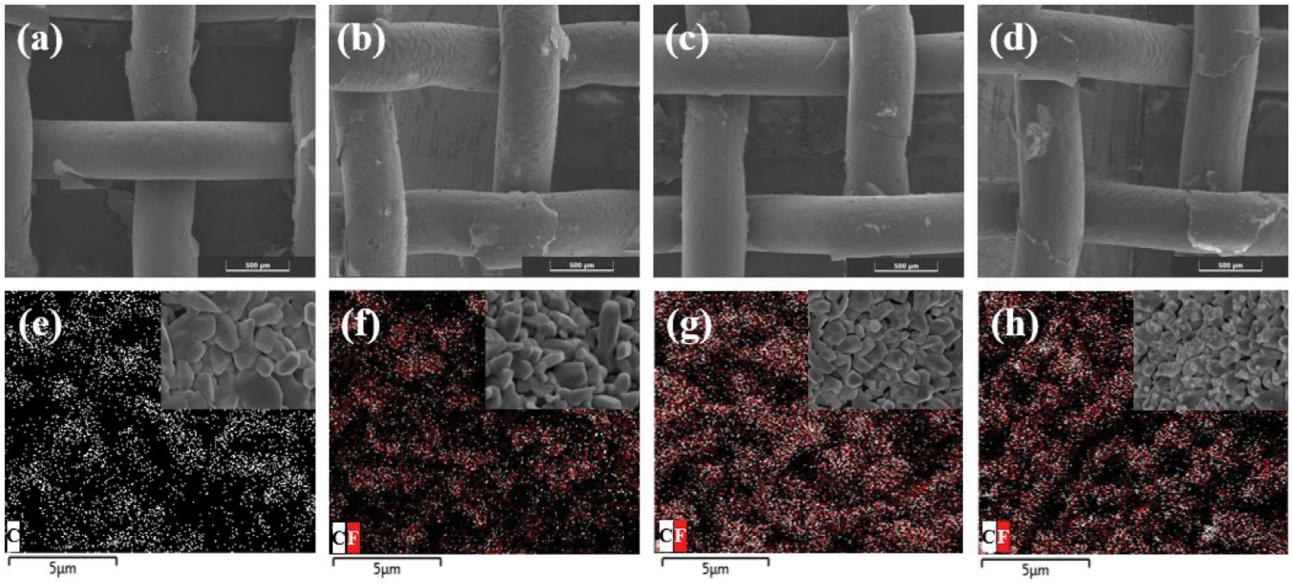

Fig. 1. FE-SEM image of (a) Mesh@C, (b) Mesh@C-F01, (c) Mesh@C-F02, and (d) Mesh@C-F03, EDS image of (e) Mesh@C, (f) Mesh@CF01, (g) Mesh@C-F02, and (h) Mesh@C-F03.

in a row. At this time, the change in separation yield and separation efficiency for ten times was evaluated. The contact angles of the manufactured mesh filters before and after the experiment were compared.

RESULTS AND DISCUSSION

1. Surface Properties

Mesh@C was observed with a polarization microscope to confirm whether carbon was coated on the SUS Mesh surface through the PVD method, and the results are shown in Fig. S2. Polarization microscope photographs of SUS Mesh and Mesh@C at a magnification of 4X are shown in Fig. S2(a) and Fig. S2(b). Due to carbon coating layer, the part of the void in Mesh@C decreased by 4.7% on average compared to the SUS Mesh. And the diameter of the wire, which was 0.5 mm, increased to 0.52 mm on average. The SUS Mesh surface was finally coated with carbon having a thickness of about 100 micrometers. In addition, a polarization microscope photograph of the cross-section of Mesh@C at a magnification of 20X is shown in Fig. S2(c). Through this, a carbon coating layer was formed on the surface of the SUS mesh.

Fig. 1 shows the analysis images of FE-SEM and EDS at each manufacturing stage. The FE-SEM images of the fabricated mesh filters are Fig. 1(a)-(d), and there was no morphological difference. It can be seen in Fig. 1(e) that carbon is coated on the surface of Mesh@C through the EDS analysis image. In the case of Mesh@C-F01, Mesh@C-F02, and Mesh@C-F03, it was observed in Fig. 1(f)-(h) that fluorine atoms introduced to reduce hydrophobicity were present on the surface together with carbon atoms.

For more detailed surface chemistry analysis, XPS analysis was performed, and the results are shown in Fig. 2(a). In Fig. 2(a), a very large C1s peak was observed in Mesh@C coated with carbon, and it was confirmed that the F1s peak was additionally present in Mesh@C-F01, Mesh@C-F02, and Mesh@C-F03. As a result of the CF_4 plasma treatment through the presence of F1s peaks, a fluorine functional group was generated to the surface of the mesh filters, and the introduction of fluorine atoms was consistent with the EDS analysis result. In addition, the surface element content is shown in Table 1 based on XPS analysis. In the case of Mesh@C, the content of carbon atoms was 95.08 at.%, and most of the surface was composed of carbon, and the content of oxygen atoms was 4.92 at.%. As the fluorination reaction proceeded, the content of carbon atoms decreased to a maximum of 71.13 at.%, and the content of fluorine atoms increased to 11.05-25.03 at.%. At this time, the highest fluorine ratio was confirmed in Mesh@C-F02 at 25.03 at.%. In the case of Mesh@C-F03, which had the longest reaction time, the fluorine content ratio was reduced to 23.69 at.% compared to Mesh@C-F02.

Table 1. XPS analysis data of carbon coated, and fluorinated carbon coated SUS Mesh

Sample	Elemental content (Atomic%)			F/C ratio (%)
	C1s	O1s	F1s	
Mesh@C	95.08	4.92	-	-
Mesh@C-F01	84.34	4.61	11.05	13.10
Mesh@C-F02	71.13	3.84	25.03	35.19
Mesh@C-F03	72.14	4.17	23.69	32.84

To analyze the XPS in more detail, the C1s data was deconvolved and shown in Fig. 2(b)-(e). The composition ratio of each detailed peak is shown in Table 2. In the case of Mesh@C, peaks were observed at 284.5, 285.7, 286.5, and 290.7 eV as shown in Fig. 2(b), and these peaks are attributed to sp2C, sp3C, C-O/C-OH, and π-π*, respectively [36]. In addition, in Table 2, Mesh@C consists mostly of sp2C at 64.44%. This is considered to be because the main component of PFO coated with SUS Mesh is the aromatic hydrocarbons composed of 1-3 aromatic rings and PFO is

Table 2. Peak parameter for C1s component of Mesh@C and Fluorine Plasma treated Mesh@C

Component	Peak position (eV)	Concentration (%)			
		Mesh@C	Mesh@C-F01	Mesh@C-F02	Mesh@C-F03
sp^2C	284.5	64.44	60.20	57.16	59.16
sp^3C	285.7	8.45	8.38	10.35	9.96
C-O/C-OH	286.10	18.60	15.42	7.92	6.41
pi-pi*	290.70	8.51	-	-	-
C-F	288.5	-	12.25	17.24	19.57
$C-F_2$	291	-	2.10	5.51	3.23
$C-F_3$	293.2	-	1.65	1.82	1.67

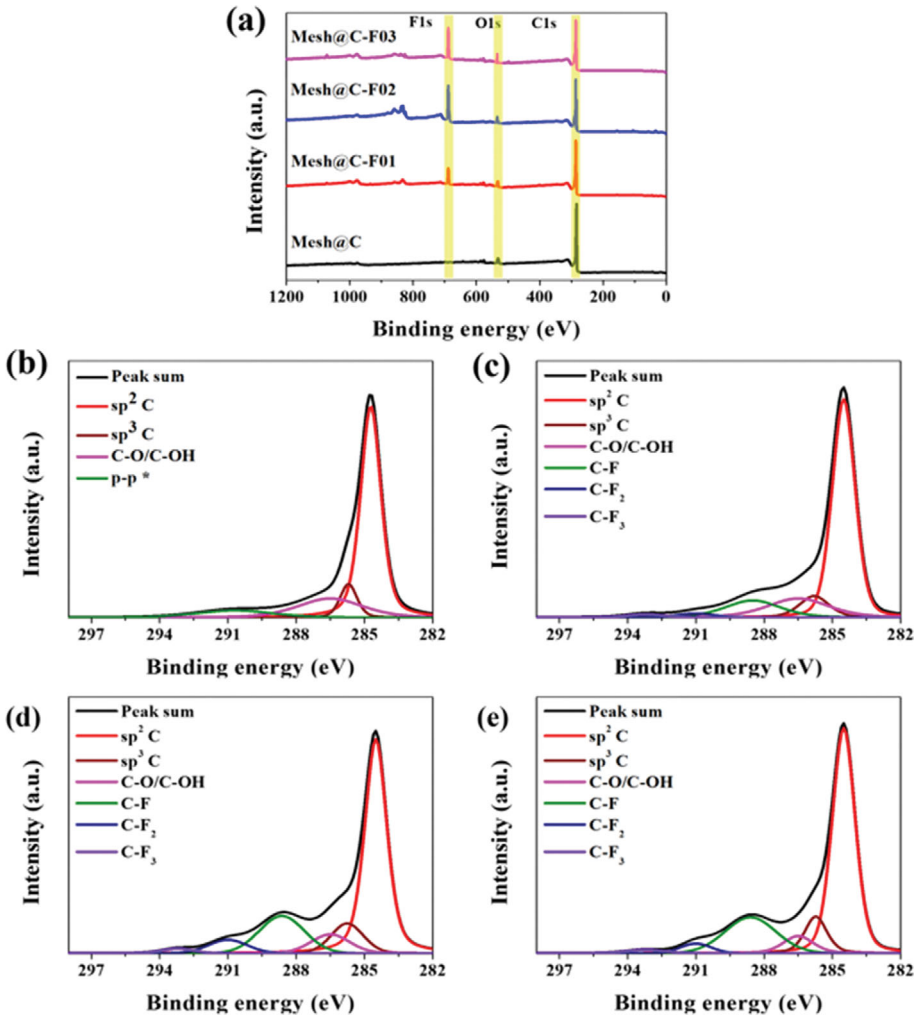

Fig. 2. (a) XPS wide scan spectra, XPS C1s spectra of (b) Mesh@C, (c) Mesh@C-F01, (d) Mesh@C-F02, and (e) Mesh@C-F03.

composed of sp2 bonded carbon [35]. In the case of Mesh@C-F01, Mesh@C-F02, and Mesh@C-F03, according to Fig. 2(c)-(d), peaks were observed at 288.5, 291, and 293.2 eV positions, which are not observed in the existing Mesh@C. These peaks refer to the peaks of the C-F, $C-F_2$, and $C-F_3$ groups, respectively [37,38]. At this time, looking at the composition ratio of the constituent peaks, the C-F, $C-F_2$ and $C-F_3$ groups all increased in Mesh@C-F02 compared to Mesh@C-F01. On the other hand, in Mesh@C-F03, C-F groups increased, but $C-F_2$ and $C-F_3$ groups decreased compared to Mesh@C-F02. It is thought that this is because the fluorine radicals additionally generated due to the long reaction time reacted with the fluorine of the previously generated fluorine functional groups (C-F, $C-F_2$ and $C-F_3$ groups) or broke the C-C bond and were released in the form of F_2 gas or CH_nF_m [33,34].

$C-F_2$ and $C-F_3$ groups improve hydrophobicity because of their low surface free energy. On the other hand, functional groups of

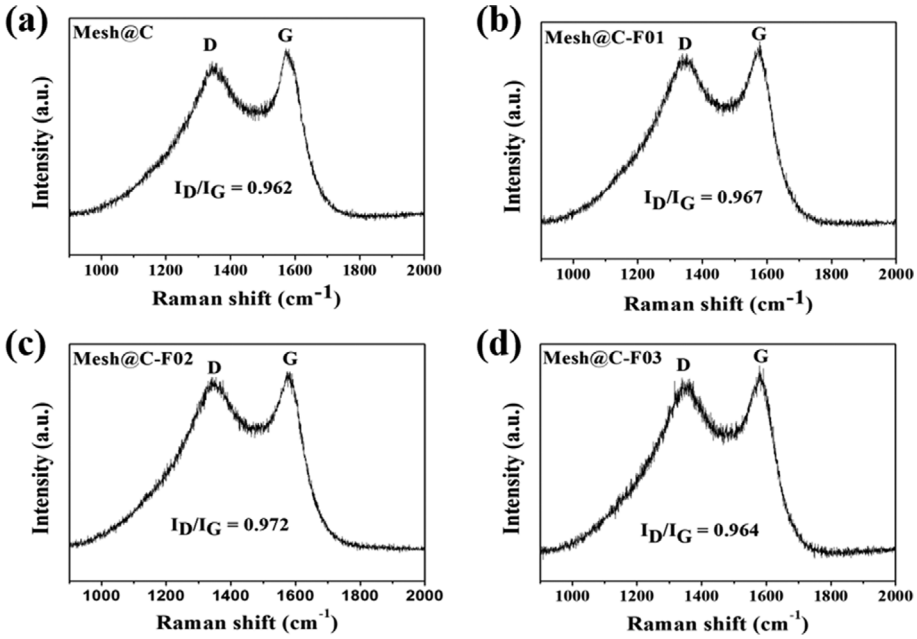

Fig. 3. Raman spectra of (a) Mesh@C, (b) Mesh@C-F01, (c) Mesh@C-F02, and (d) Mesh@C-F03.

C-F groups such as -CH_2-CHF- have relatively higher surface free energy than hydrocarbon groups [33,34,39]. Therefore, it was confirmed through the XPS analysis result that Mesh@C-F02, which had the highest ratio of C-F_2 and C-F_3 groups, improved the hydrophobicity the most among the manufactured mesh filters.

Raman analysis was performed to confirm the structural change of the coated carbon layer according to the fluorination time. The results of Raman analysis measured in the range of 900 cm^{-1} to 2,000 cm^{-1} are shown in Fig. 3, and the irradiated laser wavelength is 514 nm. The peaks observed in the range of 1,338.02 cm^{-1} to 1,343.31 cm^{-1} in Fig. 3 indicate defects in the carbon structure, which is called the D peak. In addition, the peaks observed in the range of 1,572.22 cm^{-1} to 1,578.24 cm^{-1} mean the degree of plane growth of the carbon structure due to the sp2 bond of carbon, which is called the G peak. The I_D/I_G value, which is a relative intensity ratio between the D and G peaks, is a measure to confirm the difference between the growth and defects of the graphite structure [40,41]. The I_D/I_G values of Mesh@C, Mesh@C-F01, Mesh@C-F02, and Mesh@C-F03 were 0.962, 0.967, 0.972, and 0.964, respectively, with no significant difference and within the error range. It is considered that there is no difference in the structure of the carbon layer when fluorine is introduced into the carbon layer of Mesh@C.

2. Water Contact Angle

Fig. 4 shows the change of WCA according to each manufacturing step and fluorination time. In the case of untreated SUS mesh, the average WCA was 101.86°. In the case of Mesh@C after carbon coating, the average WCA was 120.41°, which increased by 18.21% compared to SUS Mesh. From this result, the carbon coating layer is expected to increase the surface hydrophobicity of the mesh filter.

Meanwhile, the average values of WCA after fluorination were 127.20°, 129.53°, and 128.29° in Mesh@C-F01, Mesh@C-F02, and Mesh@C-F03. At this time, the highest WCA was observed in Mesh@C-F02, and the average value increased by 27.20% compared to that of SUS Mesh. Looking at the change in WCA according to the fluorination conditions, Mesh@C-F03, which had a longer fluorination reaction time, had a lower WCA than Mesh@C-F02. The wettability of the mesh filters manufactured in this way is due to the change in the surface chemical composition by fluorination treatment, and the largest WCA of Mesh@C-F02 is consistent with the XPS result. In this plasma fluorination test condition, it was found that it was difficult to directly fluoride the mesh filter. It is evaluated that the coated carbon layer serves to improve hydrophobicity and works as a base film for fluorination at the same time.

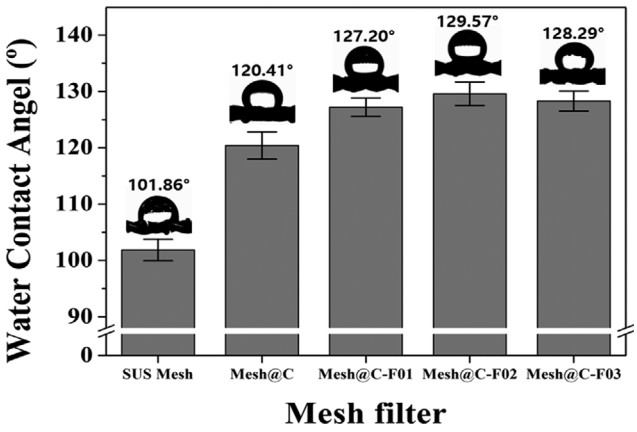

Fig. 4. Change of water contact angle for each sample.

3. Oil/Water Separation

After performing an oil/water separation experiment for two minutes using SUS Mesh, Mesh@C, and Mesh@C-F02, the separation yield and separation efficiency were calculated, and the results

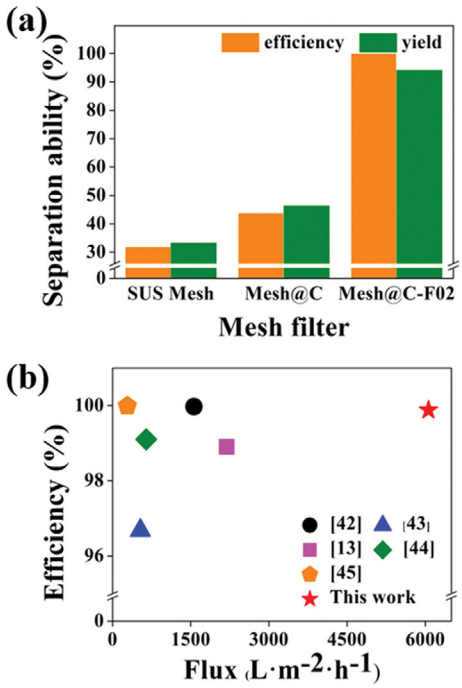

Fig. 5. (a) Separation efficiency of oil and water for 2 minutes in each manufacturing step, (b) efficiency and flux comparison with other previous studies that conducted oil/water separation experiments using soybean oil.

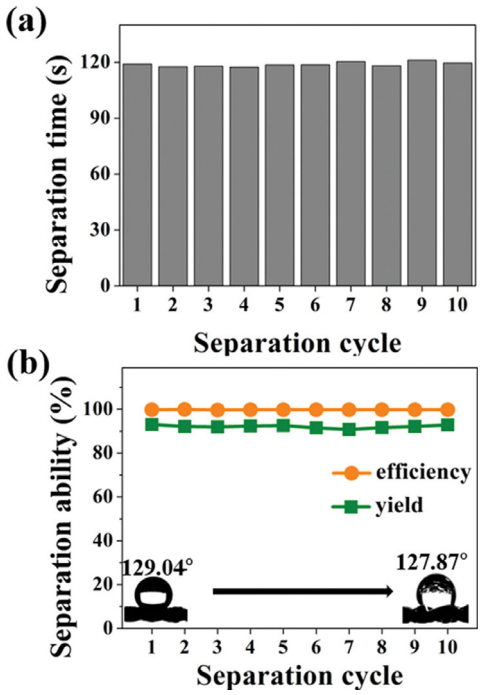

Fig. 6. (a) The time it takes for no more separation to occur in each separation cycle, (b) changes in separation efficiency and yield during continuous separation (10 times), and change in water contact angle.

are shown in Fig. 5(a). The SUS Mesh and Mesh@C used in this experiment had low hydrophobicity, and the separation efficiency was very low because DI water and soybean oil could not be separated. On the other hand, in the case of Mesh@C-F02, whose hydrophobicity was improved through fluorine plasma treatment, the separation ability was observed to be very high. The purity of the water in the remaining right bath was 94.06 wt%, and the purity of the oil in the separated solution was 99.88 wt%. That is, the separation yield was 94.06%, and high separation efficiency of 99.88% was observed. The results of the oil/water separation experiment of Mesh@C-F02 are shown in Fig. S3. Mesh@C-F02 separated water and soybean oil very quickly, and no further change was observed in less than two minutes. Based on these results, Mesh@C-F02 is expected to be applied as an oil/water separation material as a mesh filter with high selectivity and rapidity.

The flux was calculated from the oil/water separation results using Mesh@C-F02 and compared with the previous study of oil/water separation materials using soybean oil; it is summarized in Fig. 5(b) [13,42-45]. The mesh filter manufactured in this experiment had more than twice the flux (6,062 $Lm^{-2}h^{-1}$) compared to the oil/water separation material manufactured in other experiments. In addition, the separation efficiency was 99.88%, which was high compared to previously published articles. Such excellent flux and high separation efficiency are attributed to the use of SUS mesh with large aperture size and improved hydrophobicity by the generation of fluorine functional groups. The separation efficiencies of reduced graphene oxide polyphenylene sulfide fibrous membrane and poly(vinylidene fluoride) membrane were as high as 99.97% and 99.99%, but the flux was very low at 1,562 $Lm^{-2}h^{-1}$ and 282 $Lm^{-2}h^{-1}$ [42,45]. In addition, their manufacturing process is relatively complicated compared to this study, and they have disadvantages in stability. Therefore, the oil/water separation material prepared in this study can be manufactured simply, and it is evaluated as an excellent oil/water separation material because it has high separation efficiency and high flux.

In addition, to evaluate the continuous oil/water separation ability, the experiment was performed ten times in a row. At this time, the change of each separation time is shown in Fig. 6(a). In addition, the change in separation yield and separation efficiency of the solution obtained after separation in ten oil/water separation processes and the change in WCA before and after the experiment of Mesh@C-F02 used are shown in Fig. 6(b). During the ten consecutive separations, the separation times were all as fast as about two minutes. The average separation yield was 92.09%, and the average separation efficiency was observed to be 99.76%. The mesh filter used at this time can confirm that the initial WCA, which was 129.57°±2, maintains hydrophobicity at 128.27°±1 after ten consecutive oil/water separation experiments. In this continuous oil/water separation experiment, Mesh@C-F02 has excellent reusability and maintains excellent selectivity and speed.

CONCLUSION

After carbon coating on SUS mesh by PVD method using PFO as a carbon precursor, hydrophobic oil/water separation material on the surface was prepared through fluorine plasma treatment. The water contact angle was confirmed to be the highest in Mesh@C-F02, which was subjected to fluorine plasma reaction for two min-

utes. It is considered that the hydrophobicity increased as the content of the C-F_2 and C-F_3 groups increased. As a result of an oil/water separation experiment with Mesh@C-F02 with improved hydrophobicity due to the generation of fluorine functional groups, a high separation efficiency of 99.88% was confirmed. Also, due to the large aperture size, 500 mL of water and oil mixture was separated in two minutes, and it was confirmed that it had a relatively large flux (6,062 $Lm^{-2}h^{-1}$) compared to other studies. Therefore, Mesh@C-F02 manufactured by a relatively simple method is evaluated as a promising oil/water separation material that separates oil and water with excellent selectivity and rapidity.

ACKNOWLEDGEMENTS

This work was supported by Industrial Strategic Technology Development Program (20012763, development of petroleum residue-based porous adsorbent for industrial wastewater treatment) funded by the Ministry of Trade, Industry & Energy (MOTIE, Korea).

SUPPORTING INFORMATION

Additional information as noted in the text. This information is available via the Internet at http://www.springer.com/chemistry/journal/11814.

REFERENCES

1. S. Huang, R. H. A. Ras and X. Tian, *Curr. Opin. Colloid Interface Sci.*, **36**, 90 (2018).
2. W. Kang, M. Li, H. Yang, X. Kang, F. Wang, H. Jiang, M. Zhang, T. Zhu and B. Sarsenbekuly, *J. Ind. Eng. Chem.*, **93**, 415 (2021).
3. I. B. Ivshina, M. S. Kuyukina, A. V. Krivoruchko, A. A. Elkin, S. O. Makarov, C. J. Cunningham, T. A. Peshkur, R. M. Atlas and J. C. Philp, *Environ. Sci.: Process. Impacts*, **17**, 120 (2015).
4. V. Broje and A. A. Keller, *Environ. Sci. Technol.*, **40**, 791 (2006).
5. N. Syed, J. Huang and Y. Feng, *Carbon Lett.*, **32**, 81 (2022).
6. S. Basak, J. Nanda and A. Banerjee, *J. Mater. Chem.*, **22**, 11658 (2012).
7. S. Chen, W. Li, F. Li, T. Li and W. Cao, *J. Ind. Eng. Chem.*, **80**, 33 (2019).
8. C.-J. Wang, W.-F. Kuan, H.-P. Lin, Y. A. Shchipunov and L.-J. Chen, *J. Ind. Eng. Chem.*, **96**, 144 (2021).
9. Q. Wang, Z. Yu, X. Zhu, Q. Xiang, H. Chen and Y. Pang, *J. Ind. Eng. Chem.*, **115**, 314 (2022).
10. Y. O. Raji, M. H. D. Othman, N. A. H. S. Nordin, M. R. Adam, Z. S. Tai, J. Usman and A. F. Ismail, *Korean J. Chem. Eng.*, **37**, 1631 (2020).
11. S. Jo and Y. Kim, *Korean J. Chem. Eng.*, **33**, 3203 (2016).
12. Z. Li, T. Shi, T. Zhang, Q. Guo, F. Qiu, X. Yue and D. Yang, *Korean J. Chem. Eng.*, **36**, 92 (2019).
13. K. Y. Eum, I. Phiri, J. W. Kim, W. S. Choi, J. M. Ko and H. Jung, *Korean J. Chem. Eng.*, **36**, 1313 (2019).
14. Z. Li and Z. Guo, *Mater. Des.*, **196**, 109144 (2020).
15. F. R. Sultanov, C. Daulbayev, B. Bakbolat, Z. A. Mansurov, A. A. Urazgaliyeva, R. Ebrahim, S. S. Pei and K.-P. Huang, *Carbon Lett.*, **30**, 81 (2020).
16. Y. Jiang, S. Wan, W. Zhao, W. Yu, S. Wang, Z. Yu, Q. Yang, W. Zhou and X. Liu, *Carbon Lett.*, **32**, 1047 (2022).
17. Z. Chu, Y. Feng and S. Seeger, *Angew. Chem. Int. Ed.*, **54**, 2328 (2015).
18. Z. Xue, Y. Cao, N. Liu, L. Feng and L. Jiang, *J. Mater. Chem. A*, **2**, 2445 (2014).
19. B. Wang, W. Liang, Z. Guo and W. Liu, *Chem. Soc. Rev.*, **44**, 336 (2015).
20. M. Zhu, Y. Liu, M. Chen, Z. Xu, L. Li and Y. Zhou, *J. Pet. Sci. Eng.*, **205**, 108889 (2021).
21. J. Wang, Y. K. Park and Y. M. Jo, *J. Ind. Eng. Chem.*, **89**, 400 (2020).
22. A. S. Singh, S. Jindani, B. Ganguly and A. V. Biradar, *J. Ind. Eng. Chem.*, **112**, 218 (2022).
23. Y. Liu, L. Wang, H. Lu and Z. Huang, *ACS Appl. Polym. Mater.*, **2**, 4770 (2020).
24. J.-H. Kim, S. Lee and Y.-S. Lee, *J. Ind. Eng. Chem.*, **27**, 307 (2015).
25. S. Sriram, R. K. Singh and A. Kumar, *Mater. Today: Proc.*, **26**, 2495 (2020).
26. S. Gbewonyo, S. Xiu, A. Shahbazi and L. Zhang, *Carbon Lett.*, **30**, 289 (2020).
27. D. Kim, K. H. Kim, C. Lim and Y.-S. Lee, *Carbon Lett.*, **32**, 321 (2022).
28. A. A. Voznesenskaya, A. V. Zhdanov and L. V. Belyaev, *Mater. Today: Proc.*, **19**, 2270 (2019).
29. K. H. Kim, J. H. Cho, J. U. Hwang, J. S. Im and Y.-S. Lee, *J. Ind. Eng. Chem.*, **99**, 48 (2021).
30. S. Ha, C. Lim and Y.-S. Lee, *J. Ind. Eng. Chem.*, **111**, 1 (2022).
31. S. Kim, C. Lim, D. Kim and Y.-S. Lee, *Appl. Chem. Eng.*, **32**, 653 (2021).
32. D. Kim, R. Mauchauffé, J. Kim and S. Y. Moon, *Sci. Rep.*, **11**, 1 (2021).
33. S. Kirk, M. Strobel, C.-Y. Lee, S. J. Pachuta, M. Prokosch, H. Lechuga, M. E. Jones, C. S. Lyons, S. Degner and Y. Yang, *Plasma Process. Polym.*, **7**, 107 (2010).
34. Y. Yang, M. Strobel, S. Kirk and M. J. Kushner, *Plasma Process. Polym.*, **7**, 123 (2010).
35. D. An, K. H. Kim, J. G. Kim and Y.-S. Lee, *Appl. Chem. Eng.*, **30**, 297 (2019).
36. J.-C. E. Yang, M.-P. Zhu, D. D. Dionysiou, B. Yuan and M.-L. Fu, *Chem. Eng. J.*, **430**, 133102 (2022).
37. Y. Kim, Y. Lee, S. Han and K.-J. Kim, *Surf. Coat. Technol.*, **200**, 4763 (2006).
38. M. E. H. M. da Costa, F. L. Freire, L. G. Jacobsohn, D. Franceschini, G. Mariotto and I. R. J. Baumvol, *Diam. Relat. Mater.*, **10**, 910 (2001).
39. S. M. Mukhopadhyay, P. Joshi, S. Datta, J. G. Zhao and P. France, *J. Phys. D: Appl. Phys.*, **35**, 1927 (2002).
40. C. Lim, Y. Ko, C. H. Kwak, S. Kim and Y.-S. Lee, *Carbon Lett.*, **32**, 1329 (2022).
41. D. An, K. H. Kim, C. Lim and Y.-S. Lee, *Carbon Lett.*, **31**, 1357 (2021).
42. T. Fan, Y. Su, Q. Fan, Z. Li, W. Cui, M. Yu, X. Ning, S. Ramakrishna and Y. Long, *ACS Appl. Mater. Interfaces*, **13**, 19377 (2021).
43. S. Fan, Z. Wang, P. Liang, H. Li, Y. Zhang, W. Fan and G. Xu, *J. Mater. Res. Technol.*, **19**, 2238 (2022).
44. A. Xie, J. Cui, J. Yang, Y. Chen, J. Dai, J. Lang, C. Li and Y. Yan, *J. Mater. Chem. A*, **7**, 8491 (2019).
45. M. Tao, L. Xue, F. Liu and L. Jiang, *Adv. Mater.*, **26**, 2943 (2014).

Supporting Information

High-efficiency oil/water separation of hydrophobic stainless steel Mesh filter through carbon and fluorine surface treatment

Seongjae Myeong*, Chaehun Lim*, Seokjin Kim*, and Young-Seak Lee*,,†**

*Department of Chemical Engineering and Applied Chemistry, Chungnam National University, 99 Daehak-ro, Yuseong-gu, Daejeon 34134, Korea
**Institute of Carbon Fusion Technology (InCFT), Chungnam National University, 99 Daehak-ro, Yuseong-gu, Daejeon 34134, Korea
(*Received 8 September 2022 • Revised 19 October 2022 • Accepted 31 October 2022*)

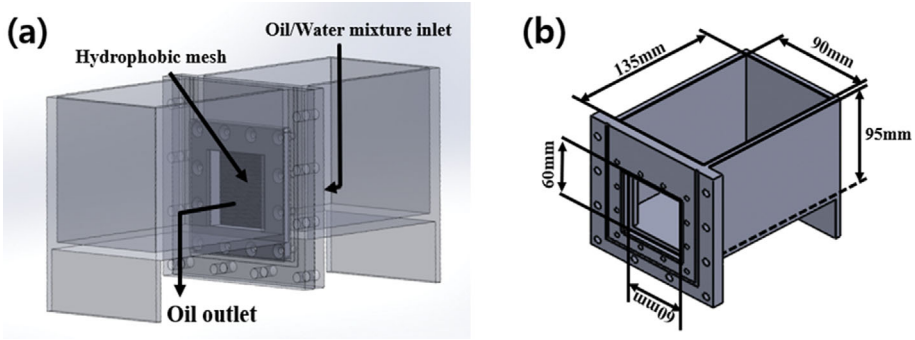

Fig. S1. Picture and size of manufactured oil/water separation equipment.

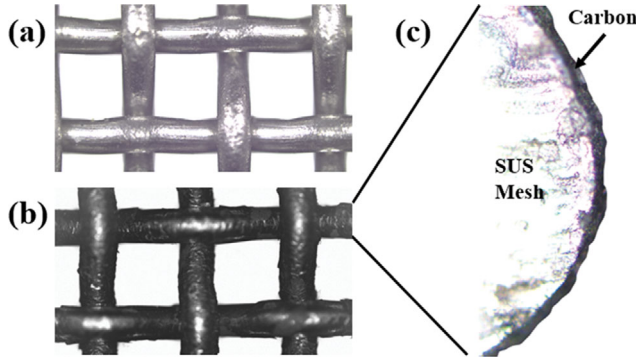

Fig. S2. Surface of (a) SUS Mesh and (b) Mesh@C through polarization microscopy, (c) TEM analysis of coated carbon layers.

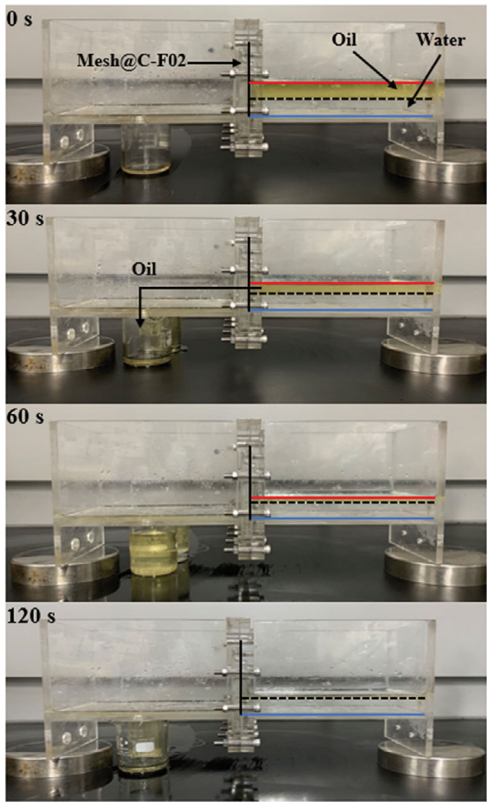

Fig. S3. Oil/water separation process for 2 minutes using the manufactured Mesh@C-F02.